Parameterization of Eddy Fluxes near Oceanic Boundaries

RAFFAELE FERRARI

Massachusetts Institute of Technology, Cambridge, Massachusetts

JAMES C. MCWILLIAMS

University of California, Los Angeles, Los Angeles, California

VITTORIO M. CANUTO

NASA Goddard Institute for Space Studies, and Department of Applied Mathematics and Physics, Columbia University, New York, New York

MIKHAIL DUBOVIKOV

NASA Goddard Institute for Space Studies, New York, New York

(Manuscript received 24 May 2006, in final form 12 September 2007)

ABSTRACT

In the stably stratified interior of the ocean, mesoscale eddies transport materials by quasi-adiabatic isopycnal stirring. Resolving or parameterizing these effects is important for modeling the oceanic general circulation and climate. Near the bottom and near the surface, however, microscale boundary layer turbulence overcomes the adiabatic, isopycnal constraints for the mesoscale transport. In this paper a formalism is presented for representing this transition from adiabatic, isopycnally oriented mesoscale fluxes in the interior to the diabatic, along-boundary mesoscale fluxes near the boundaries. A simple parameterization form is proposed that illustrates its consequences in an idealized flow. The transition is not confined to the turbulent boundary layers, but extends into the partially diabatic transition layers on their interiorward edge. A transition layer occurs because of the mesoscale variability in the boundary layer and the associated mesoscale–microscale dynamical coupling.

1. Introduction

Eddy fluxes of momentum, buoyancy, and material tracers exert a profound influence on the oceanic general circulation and its associated material distributions. These fluxes must be represented in modern oceanic general circulation models (OGCMs) and climate models where the oceanic horizontal grid resolution is usually $O(100)$ km or larger. At this resolution all the mesoscale and microscale fluxes are subgrid scale, and their transport effects must be parameterized. Although more powerful computers may soon decrease the feasible grid scale to a marginal mesoscale eddy resolution of $O(25)$ km, even finer grids of $O(10)$ km or better are needed to adequately resolve the fluxes produced by mesoscale motions (Paiva et al. 1999; Smith et al. 2000). Furthermore, even marginal eddy resolution requires some parameterization of the missing eddy fluxes (Roberts and Marshall 1998). This problem has elicited a large literature on mesoscale parameterization schemes in the oceanic interior, in addition to an even larger literature on parameterization of microscale turbulent fluxes in the planetary boundary layers (BLs). At present the parameterizations do not account consistently for interactions between mesoscale and microscale turbulence. The goal of this paper is first to review what is known about feedbacks of microscale turbulence on mesoscale eddy fluxes and then to present a parameterization framework that accounts for these interactions in the top and bottom near-boundary regions.

Mesoscale parameterizations used in OGCMs repre-

Corresponding author address: Raffaele Ferrari, Department of Earth, Atmospheric, and Planetary Sciences, Massachusetts Institute of Technology, 54-1420, 77 Massachusetts Avenue, Cambridge, MA 02139.
E-mail: rferrari@mit.edu

DOI: 10.1175/2007JCLI1510.1

sent the adiabatic release of potential energy by baroclinic instability, as suggested by Gent and McWilliams (1990, hereafter GM), the stirring and mixing of material tracers along isopycnal surfaces, and momentum transport by lateral Reynolds stress (e.g., Smith and McWilliams 2003). Their quasi-adiabatic, material conservation properties have yielded significant improvements in OGCM solutions (Danabasoglu et al. 1994). However, this parameterization framework breaks down close to the top and bottom boundaries where mesoscale eddy fluxes develop a diabatic component, both because of the vigorous microscale turbulence in BLs and because geostrophic eddy motions are constrained to follow the boundary (i.e., bottom topography or upper free surface), while the isopycnal surfaces often intersect the boundaries. Griffies (2004) reviews the main deficiencies of the adiabatic formalism at the boundaries. First, adiabatic parameterizations, like in GM produce very large tracer transports in the oceanic BLs in disagreement with observations and eddy-resolving numerical experiments. Second, the adiabatic parameterization does not include any diabatic flux of heat and salt, which are known to play an important role in the heat and freshwater budgets at strong oceanic currents, like the Antarctic Circumpolar Current (Hallberg and Gnanadesikan 2006). A different paradigm is necessary to extend eddy parameterizations into the BLs.

Previous discussions of mesoscale eddy parameterizations near boundaries argue that the normal component of an eddy flux must vanish at the boundary, even though tangential advective and diffusive components are allowable and even desirable (Danabasoglu and McWilliams 1995; Large et al. 1997; Treguier et al. 1997; McDougall and McIntosh 2001; Killworth 2001). However, no explicit parameterization forms are presented in these works. Common practice in ocean models has been to adopt ad hoc tapering functions to turn off the GM parameterization at the boundaries. This approach has the advantage of eliminating spurious BL transports, but it does not result in parameterization for mesoscale eddy fluxes within the BLs, except for the spurious effects due to tapering. This is at odds with the observational evidence that eddy fluxes have a strong impact both on the material composition and exchange rate between the surface BL and pycnocline and on the air–sea fluxes of heat (Robbins et al. 2000; Price 2001; Weller 2003).

More recently Greatbatch and Li (2000) and Griffies (2004) have proposed parameterizations that include eddy transport in the BL. The parameterizations differ in some details, but in both cases the basic idea is to extend the interior eddy transport into the BLs through analytic continuation of the interior parameterization formulas. This is essentially the same argument originally proposed by Treguier et al. (1997). In this paper we extend the approach of Treguier et al. to explicitly account for the properties of the eddy fluxes within the BLs; that is, we derive formulas for the eddy-induced transports that depend on the local eddy fluxes. We then use physical arguments about eddy statistics in the upper ocean to derive a BL parameterization. A major advantage of our approach is that it provides expressions that can be checked versus high-resolution numerical simulations. The analytical continuation approach does not provide any guidance on how to validate the parameterization.

Climate models are known to be sensitive to the treatment of mesoscale eddy fluxes in the BLs (Griffies 2004; Gnanadesikan et al. 2007). Consider as an illustrative example the upper-ocean temperature difference between two global numerical simulations that both use the GM scheme to parameterize mesoscale eddies but adopt two different tapering functions to turn off eddy transport in the BLs (Fig. 1). The two simulations are run with the Massachusetts Institute of Technology (MIT) OGCM (Marshall et al. 1997) and are identical in everything (i.e., parameters, initial conditions, boundary conditions, forcing, and parameterization schemes) except that one uses the tapering scheme proposed by Gerdes et al. (1991) and the other uses the tapering scheme suggested in Danabasoglu and McWilliams (1995). The two tapering schemes produce sea surface temperature differences as large as a few degrees in regions where the models have strong heat exchange with the atmosphere (e.g., western boundary currents and the Antarctic Circumpolar Current). There is no obvious pattern to suggest that one solution is superior to the other. They both suffer from biases generated by an improper treatment of eddy fluxes in the BL.

The goal of this paper is to derive a simple closure scheme that accounts for diabatic eddy transports in the BLs, but does not suffer from the arbitrariness of present tapering functions or heuristic arguments based on quasigeostrophic theory inappropriate for the BL (e.g., Treguier et al. 1997). In section 2 we discuss guiding principles for the structure of mesoscale and microscale fluxes near the oceanic boundaries. We argue that there must be a vertical transition layer that separates the quasi-adiabatic interior and the diabatic BL. This transition region plays an important role in the exchange of properties between the boundaries and the interior, and we make it an explicit part of the parameterization scheme. Explicit parameterization formulas that represent the eddy transports in all three regions

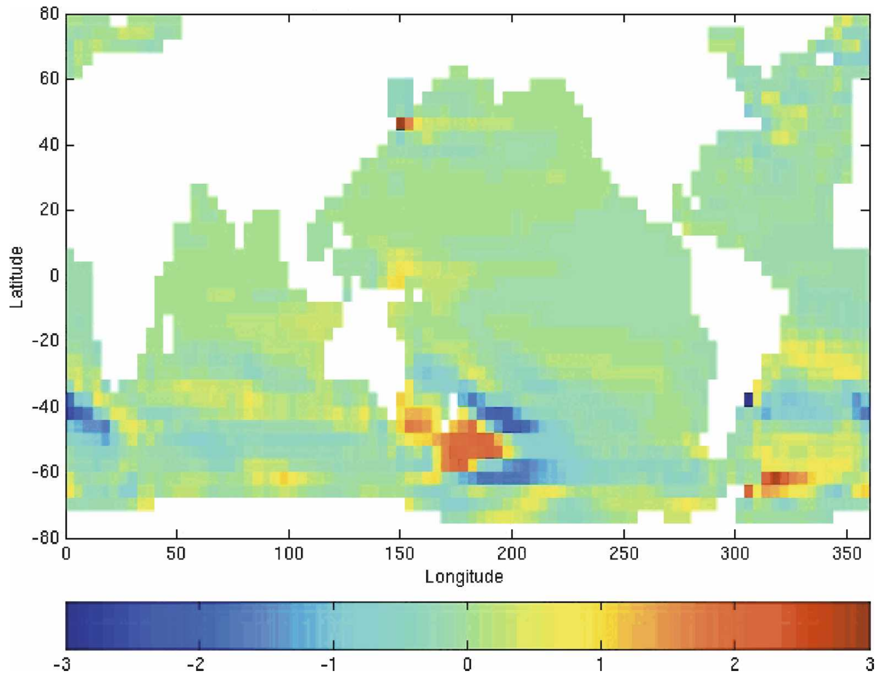

FIG. 1. Temperature differences at 170 m between two equilibrated climate simulations run with the MIT OGCM. The simulations are identical except for the use of different tapering functions applied to the GM scheme. The two tapering functions used are those proposed by Danabasoglu and McWilliams (1995) and Gerdes et al. (1991) and described in section 5. The GM schemes use a diffusivity of $\kappa_{GM} = 1000\ m^2\ s^{-1}$. The simulations are run for 1000 years with a horizontal resolution of 4°. (Simulations run by Alistair Adcroft.)

are given in section 3. In section 4 we illustrate some of the implications of our parameterizations in an idealized circulation. Finally, in section 5 we present our conclusions. The implementation and impact of these parameterizations in a global oceanic model is the topic of a separate paper (Danabasoglu et al. 2008).

2. Mesoscale and microscale fluxes in the general circulation

The oceanic general circulation is significantly affected by a variety of processes occurring at space and time scales too small to be resolved explicitly in OGCMs, and their influences need to be parameterized with variables that are explicitly included in the models. In terms of a Reynolds decomposition of variables into a slowly changing "mean" and fluctuation components, we seek a representation of the eddy fluxes $\overline{u_i'c'}$ for scalar variables c (including buoyancy) and $\overline{u_i'u_j'}$ for momentum, where the prime superscript denotes a fluctuation and the overbar denotes an average over fluctuations. It is physically sensible to further separate the fluctuations in two dynamical classes: the "momentum balanced" mesoscale eddies (McWilliams 2003) and the microscale "unbalanced" turbulence (Joyce 1977; Davis 1994; Garrett 2001). This suggests using a triple decomposition of variables into mean, mesoscale, and microscale components and writing $c = c_m + c_e + c_t$ with subscripts m, e, and t denoting the mean, mesoscale, and microscale, respectively. Angle brackets will indicate large-scale averages; that is, $c_m = \langle c \rangle$. The mean balance for any advectively conserved tracer c has the following form in terms of the triple decomposition:

$$\partial_t c_m + \mathbf{u}_m \cdot \boldsymbol{\nabla} c_m = -\boldsymbol{\nabla} \cdot \langle \mathbf{u}_e c_e \rangle - \boldsymbol{\nabla} \cdot \langle \mathbf{u}_t c_t \rangle + \mathscr{C}_m \quad (1)$$

in which $\mathscr{C}_m$ represents the mean sources and sinks of c explicitly resolved in models. In large-scale OGCMs that do not adequately resolve the eddies, parameterizations are needed for both mesoscale and microscale tracer fluxes on the right side of (1). An analogous issue arises in the mean momentum balance where parameterizations are needed for mesoscale and microscale Reynolds stresses.

Equations such as (1) are valid under the assumption that there are spectral gaps among mean, mesoscale, and microscale components, so that correlations between fluctuations on different scales can be neglected. A gap plausibly exists between mesoscale, momentum-balanced currents and microscale, unbalanced turbulence, such as breaking internal waves, shear instability, double diffusion, and mixing in the surface and bottom BLs. It is less clear that such a gap exists between the large-scale circulation and the mesoscale eddies (Scott and Wang 2005). Nonetheless, a dynamical gap does exist, and it is given an operational definition by the choice of an OGCM's horizontal resolution and eddy diffusivities. A coarsely resolved, diffusive OGCM has a mean circulation but no eddies, while a finely resolved OGCM with a more advective circulation produces vigorous mesoscale eddies (though they may be difficult to resolve accurately). This distinction allows us to talk separately about mean and eddy motions.

In the oceanic modeling literature eddy parameterizations are usually derived under the assumption that mesoscale and microscale fluxes act independently. The justification is that mesoscale eddies represent the adiabatic rearrangement of buoyancy surfaces and tracers under the influences of gravity and rotation, while microscale turbulence controls all the irreversible, diabatic processes that modify the buoyancy and tracer concentrations of the water parcels. The microscale turbulent fluxes are typically parameterized as vertical downgradient with Fickian laws both for momentum and for tracers (Gregg et al. 2003). The diffusivities κ and viscosities ν are set to small, albeit climatically important, values in the oceanic interior, consistent with direct measurements (Ledwell et al. 1993; Toole et al. 1994). Turbulence is intensified near the oceanic boundaries by boundary fluxes (i.e., wind stress and buoyancy fluxes at the surface and drag at the bottom) and consequent flow instabilities. This turbulence generates overturning motions that often make the buoyancy and velocity profiles well mixed in the BL. Traditional BL models (e.g., Kraus and Turner 1967; Mellor and Yamada 1974; Price et al. 1986; Large at al. 1994) represent these fluxes with vertical profiles for $\kappa(z)$ and $\nu(z)$ that are strongly enhanced compared to interior values.

The parameterization of mesoscale eddy fluxes is still in its infancy. Most formulations are local in the sense that the eddy term is calculated with local values and gradients of the resolved quantities. The few exceptions to the rule include parameterizations that depend on vertically integrated quantities and are therefore nonlocal in the vertical. Parameterizations are derived for eddy tracer fluxes, such as temperature, salinity, and biogeochemical quantities (GM; Greatbatch and Lamb 1990; Visbeck et al. 1997; Treguier et al. 1997; Killworth 1997), while retaining simple horizontal diffusion for eddy momentum fluxes with an eddy viscosity as small as is consistent with numerical stability. This approach has been shown to capture the most important eddy effects on the mean circulation in the limit of small Rossby numbers typically found in the ocean (Treguier et al. 1997; Drijfhout and Hazeleger 2001; Wardle and Marshall 2000). These schemes can be extended to account more accurately for eddy momentum fluxes (Wardle and Marshall 2000; Smith and McWilliams 2003; Plumb and Ferrari 2005; Ferreira et al. 2005), but experience with these extensions in OGCMs is still limited.

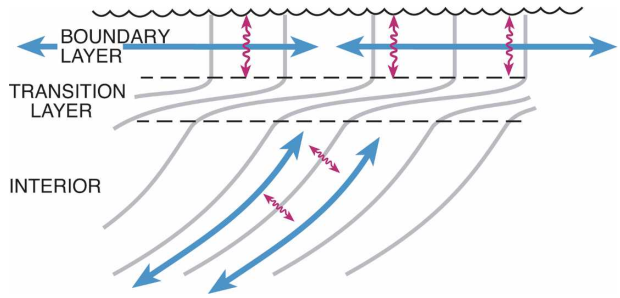

Fig. 2. A conceptual model of eddy fluxes in the upper ocean. Mesoscale eddy fluxes (blue arrows) act to both move isopycnal surfaces and stir materials along them in the oceanic *interior*, but the fluxes become parallel to the boundary and cross density surfaces within the *BL*. Microscale turbulent fluxes (red arrows) mix materials across isopycnal surfaces, weakly in the interior and strongly near the boundary. The interior and the BL regions are connected through a *transition layer* where the mesoscale fluxes rotate toward the boundary-parallel direction and develop a diabatic component.

Most of the existing mesoscale parameterization proposals (section 1) are intended for the oceanic interior where the effect of eddies is predominantly adiabatic. However, near horizontal and vertical boundaries eddies can develop diabatic behavior, and some ad hoc form of adjustment has to be made to avoid false eddy transports through the solid boundaries (Danabasoglu and McWilliams 1995; Large et al. 1997; McDougall and McIntosh 2001; Killworth 2001). We formulate a parameterization scheme that expresses the essential diabatic nature of eddy fluxes in the BLs as a modification of the existing adiabatic parameterizations. We borrow the basic framework of Treguier et al. (1997) but extend it beyond quasigeostrophic theory. As a starting point we divide the ocean into three different types of layers according to different properties of the mesoscale fluxes (Fig. 2).

a. Oceanic interior

Eddy fluxes in the oceanic interior are largely along isopycnal surfaces with a much weaker diapycnal component. Thus it is useful to project the full flux along and across the mean isopycnal surfaces and consider

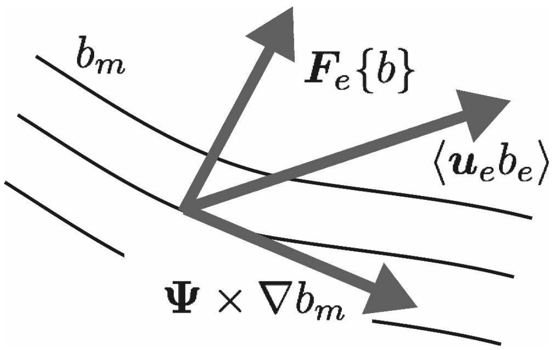

FIG. 3. Decomposition of the buoyancy eddy flux $\langle \mathbf{u}_e b_e \rangle$ into two components, *along* and *across* mean buoyancy surfaces b_m. The along-isopycnal component $\boldsymbol{\Psi} \times \boldsymbol{\nabla} b_m$ represents the advective skew flux, while the across-isopycnal component $\mathbf{F}_e\{b\}$ represents the diapycnal residual flux.

the two components separately (Andrews and McIntyre 1978; Ferrari and Plumb 2003),

$$\langle \mathbf{u}_e b_e \rangle = -\frac{\langle \mathbf{u}_e b_e \rangle \times \boldsymbol{\nabla} b_m}{|\boldsymbol{\nabla} b_m|^2} \times \boldsymbol{\nabla} b_m + \frac{\langle \mathbf{u}_e b_e \rangle \cdot \boldsymbol{\nabla} b_m}{|\boldsymbol{\nabla} b_m|^2} \boldsymbol{\nabla} b_m, \tag{2}$$

where b is buoyancy. The decomposition is shown in Fig. 3. After taking its divergence, the cross-gradient flux component—the so-called *skew flux*—is equivalent to a mean buoyancy advection,

$$\boldsymbol{\nabla} \cdot \left(\frac{\langle \mathbf{u}_e b_e \rangle \times \boldsymbol{\nabla} b_m}{|\boldsymbol{\nabla} b_m|^2} \times \boldsymbol{\nabla} b_m \right) = \left(\boldsymbol{\nabla} \times \frac{\langle \mathbf{u}_e b_e \rangle \times \boldsymbol{\nabla} b_m}{|\boldsymbol{\nabla} b_m|^2} \right) \cdot \boldsymbol{\nabla} b_m. \tag{3}$$

The nondivergent, eddy-induced velocity $\mathbf{u}_{me}$ is given by the curl of the vector streamfunction $\boldsymbol{\Psi}$:

$$\mathbf{u}_{me} = \boldsymbol{\nabla} \times \boldsymbol{\Psi}, \quad \boldsymbol{\Psi} \equiv -\frac{\langle \mathbf{u}_e b_e \rangle \times \boldsymbol{\nabla} b_m}{|\boldsymbol{\nabla} b_m|^2}. \tag{4}$$

The velocity $\mathbf{u}_{me}$ represents the rectified transport generated by eddies advecting buoyancy perturbations along mean isopycnal surfaces.

The residual buoyancy flux, $\mathbf{F}_e\{b\}$, is directed across mean isopycnal surfaces and represents eddy mixing of water masses with different mean buoyancy (Plumb and Ferrari 2005),

$$\mathbf{F}_e\{b\} \equiv \frac{\langle \mathbf{u}_e b_e \rangle \cdot \boldsymbol{\nabla} b_m}{|\boldsymbol{\nabla} b_m|^2} \boldsymbol{\nabla} b_m. \tag{5}$$

The buoyancy budget can then be conveniently written as

$$\partial_t b_m + (\mathbf{u}_m + \mathbf{u}_{me}) \cdot \boldsymbol{\nabla} b_m = -\boldsymbol{\nabla} \cdot \mathbf{F}_e\{b\} - \boldsymbol{\nabla} \cdot \langle \mathbf{u}_t b_t \rangle + \mathcal{B}_m. \tag{6}$$

In the oceanic interior, mesoscale eddies satisfy quasigeostrophic scaling (Treguier et al. 1997) and the expressions for the vector streamfunction and the diabatic flux at leading order in Rossby number reduce to

$$\boldsymbol{\Psi} \approx \frac{\mathbf{z} \times \langle \mathbf{u}_e b_e \rangle}{\partial_z b_m}, \quad \mathbf{F}_e\{b\} \equiv 0. \tag{7}$$

McDougall and McIntosh (2001) point out that diapycnal fluxes, despite being small, appear to be of climatic importance when estimated according to (5). However, direct measurements exclude large diapycnal fluxes in the oceanic interior and suggest that eddy fluxes must be aligned with the instantaneous isopycnals. The solution to the conundrum is that the diapycnal component is a result of averaging at a fixed vertical position instead of averaging along fixed isopycnal surfaces. McDougall and McIntosh (2001) hence propose to formulate eddy parameterizations in isopycnal coordinates. Adopting isopycnal averages, however, raises problems in the unstratified BLs because isopycnal coordinates become ill defined. Furthermore, Killworth (2001) finds that parameterizations based on isopycnal coordinates do not have more skill than z-based parameterizations that ignore residual buoyancy fluxes. We therefore proceed with a formulation in z coordinates and set the residual flux in (7) to zero.

For passive tracers $c \neq b$, there is an additional along-isopycnal residual eddy flux component in $\mathbf{F}_e\{c\} = \langle \mathbf{u}_e c_e \rangle - \boldsymbol{\Psi} \times \boldsymbol{\nabla} c_m$, whose effect on mean buoyancy is trivial. This residual flux appears at leading order in Rossby number and must be parameterized (Solomon 1971; Redi 1982).

b. Boundary layer

In the turbulent BLs the eddy flux component normal to the boundaries vanishes, so the fluxes become parallel to the boundaries. We assume that each of the normal components of mean, mesoscale, and microscale velocities vanish separately. The implication is that mesoscale eddies mix tracers along the boundaries and are not constrained to be along isopycnal surfaces. The decomposition in (2) is not very useful to progress toward eddy parameterizations in such a situation. An obvious problem is that the eddy-induced velocity and the residual flux do not individually satisfy no-normal flux boundary conditions, even though the full eddy buoyancy flux does. For a boundary with a unit normal vector $\mathbf{n}$, the normal components of the eddy-induced velocity and the residual flux are

$$\mathbf{u}_{me} \cdot \mathbf{n} = \boldsymbol{\nabla} \times \boldsymbol{\Psi} \cdot \mathbf{n}, \quad \mathbf{F}_e\{b\} \cdot \mathbf{n} = (\boldsymbol{\Psi} \times \mathbf{n}) \cdot \boldsymbol{\nabla} b_m. \tag{8}$$

Both components imply an eddy buoyancy flux *across* the boundaries whenever the vector streamfunction has a component *along* the boundaries, but they cancel when added together. The issue disappears in the presence of a well-mixed BL where $\nabla b_m \cdot \mathbf{n} \to 0$ approaching the boundary. In this case $\boldsymbol{\Psi}$ has no component along the boundary,[1] and $\mathbf{F}_e\{b\}$ is along the boundary. However, BLs can be stratified and, in such cases, one can retain the desirable property of vanishing cross-boundary eddy-induced advection by using an appropriate gauge transformation in the definition of $\boldsymbol{\Psi}$. A detailed derivation is presented in appendix A. Here we write the result for the case when the boundaries are horizontal,

$$\boldsymbol{\Psi} \equiv -\frac{\langle w_e b_e\rangle}{|\nabla_{\text{hor}} b_m|^2}\mathbf{z} \times \nabla_{\text{hor}} b_m - \frac{\langle \mathbf{u}_{he} b_e\rangle \times \nabla_{\text{hor}} b_m}{|\nabla_{\text{hor}} b_m|^2}, \tag{9}$$

$$\mathbf{F}_e\{b\} \equiv \frac{\langle \mathbf{u}_e b_e\rangle \cdot \nabla b_m}{|\nabla_{\text{hor}} b_m|^2}\nabla_{\text{hor}} b_m, \tag{10}$$

where $\mathbf{u}_{he}$ and ∇_{hor} are the horizontal components of the eddy-induced velocity and gradient operator. A similar decomposition is introduced by Held and Schneider (1999) for a zonal flow. These definitions differ from (4) and (5), but the difference is physically inconsequential because the two definitions give the same flux divergences. Most importantly, at the boundaries the first term in (9) vanishes and the eddy-induced velocity and the residual flux are horizontal. Thus, by using an appropriate gauge transformation, we have eliminated any cross-boundary advection. A generalization to arbitrary boundaries is given in appendix A. In this paper we restrict our analysis to surface and bottom BLs, both because side boundaries are computational artifacts in OGCMs (compared to coastlines in nature) and because approximate thermal wind balance and no-slip, insulating boundary conditions usually imply weak near-boundary flow.

The expressions (9) and (10) confirm that there is no physical justification to taper eddy parameterizations at the oceanic boundaries. Observations (Weller 2003) and eddy-resolving numerical simulations (Oschlies 2002) show that mesoscale fluxes penetrate into the surface BL, and neither the eddy-induced streamfunction nor the residual flux vanish. Our goal is to find guiding principles to parameterize these fluxes. As we discuss in section 3, mixing length arguments suggest that the horizontal fluxes of buoyancy are directed down the mean buoyancy gradient both in the ocean interior and at the boundaries, $\langle \mathbf{u}_{he} b_e\rangle = -\kappa_{\text{GM}}\nabla_{\text{hor}} b_m$. Substituting the downgradient closure in (9) and (10), the parameterization problem is reduced to choosing the appropriate forms for the eddy diffusivity κ_{GM} and the vertical fluxes.

Within the BLs momentum and tracers are well homogenized in the vertical as a result of all turbulent processes that actively mix the BLs on time scales shorter than the mesoscale eddy turnover times. Continuity then demands that the mesoscale vertical velocity is linear in z. Hence, we expect the mean climatological gradients $\nabla_H b_m$ and the horizontal eddy fluxes $\langle \mathbf{u}_{he} b_e\rangle$ to be constant across the BL and the vertical flux $\langle w_{he} b_e\rangle$ to be linear in z and vanish at the boundary. Both approximations are in agreement with results from the eddy-resolving numerical experiments described in Cessi et al. (2006).

Marshall (1997), Treguier et al. (1997), and Marshall and Radko (2003) assume that the eddy-induced mass exchange between the BL and the interior is continuous. These heuristic arguments have been recently verified in eddy-resolving numerical simulations (Cessi et al. 2006; Cerovecki et al. 2006, manuscript submitted to *J. Phys. Oceanogr.,* hereafter CPH). Continuity of $\boldsymbol{\Psi}$ across the BL base, together with the assumption that any along-boundary transport does not change in the across-boundary direction, implies that the vertical component of $\boldsymbol{\Psi}$ vanishes in the BL because it is zero in the interior as per (9). The horizontal component of $\boldsymbol{\Psi}$, which represents overturning circulations, must go to zero together with the vertical eddy flux. These simple rules are used in the next section to build a parameterization scheme.

The residual flux (10) is small in the oceanic interior because of a large cancellation between $\langle \mathbf{u}_{he} b_e\rangle \cdot \nabla_{\text{hor}} b_m$ and $\langle w_e b_e\rangle \partial_z b_m$. The first component does not change through the BL base, while the second component essentially vanishes because the vertical stratification becomes much weaker. As a result, in the BL there is a large residual flux in the horizontal that crosses density surfaces (Treguier et al. 1997). A schematic of the vertical structure of the eddy transport in the surface BL is shown in Fig. 4. There is no consistent treatment of these fluxes in present parameterization schemes.

In this section we argue that the eddy-induced horizontal velocities (given by the vertical derivative of $\boldsymbol{\Psi}$) and the residual fluxes are independent of depth within the BL. In the absence of any shear, mesoscale eddies cannot drive any restratification within the BL. This seems at odds with Oschlies's (2002) result that the BL depth is reduced in eddy-resolving numerical models as a result of increased surface velocity shears. However Young (1994), Haine and Marshall (1998), and Boccaletti et al. (2007) show that the enhanced shears are not

[1] The normal component of the eddy-induced velocity is given by $\nabla \cdot [\boldsymbol{\Psi} \times \mathbf{n}] - \boldsymbol{\Psi} \cdot \nabla \times \mathbf{n}$. In a well-mixed BL, the first term vanishes because $\boldsymbol{\Psi}$ is directed along $\mathbf{n}$. The second term also vanishes because $\mathbf{n} \cdot \nabla \times \mathbf{n} = 0$ for any differentiable surface (Sneddon 1957).

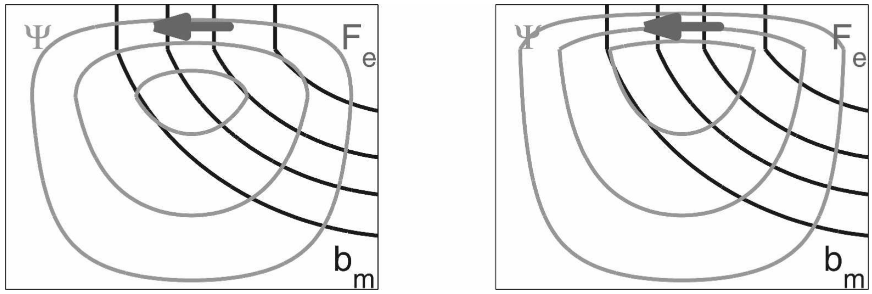

FIG. 4. Eddy-induced circulation (light gray contours) and diabatic residual flux (dark gray arrows) in the meridional plane of a hypothetical zonally averaged channel flow. The black lines represent the mean buoyancy surfaces that outcrop at the surface in response to diabatic surface fluxes. The eddy-induced circulation, based on the definition in (9), goes linearly to zero at the surface within the BL in response to the strong vertical mixing that erases mesoscale vertical shears. A diabatic flux parallel to the boundary appears at the surface, as defined in (10). (right) Matching of the eddy-induced circulation between the BL and the interior occurs through a transition layer according to the expression in (25). The streamfunction and its vertical derivative are continuous everywhere and give a continuous eddy-induced velocity. The diabatic flux acts both in the boundary and transition layers. (left) Eddy-induced circulation obtained setting the transition layer thickness to zero. A discontinuity develops in the derivative of $\boldsymbol{\Psi}$ and the associated eddy-induced velocity. Such discontinuities are unphysical and occasionally trigger convective instabilities (Griffies 2004).

associated with mesoscale eddies, but with submesoscale processes like frontogenesis and frontal instabilities within the BL. Mesoscale shear is dominated by baroclinic mode one (Wunsch 1997). Hence changes in mesoscale eddy velocity through the BL scale with the ratio of the BL depth to the vertical scale of mode one are typically less than 10% of the total velocity. For present purposes, we can safely ignore such small shears and assume that lateral mesoscale fluxes are, to leading order, depth independent.

Submesoscale eddies drive weak horizontal fluxes compared to mesoscale motions but dominate the vertical fluxes of buoyancy and tracers (Boccaletti et al. 2007). The vertical fluxes drive ageostrophic circulations that tilt isopycnals from the vertical to the horizontal and achieve restratification. Fox-Kemper and Ferrari (2008) show that submesoscale restratification can be parameterized independently of mesoscale processes with an additional eddy-induced overturning streamfunction that acts only within the BL. A treatment of submesoscale dynamics goes beyond the scope of this paper and the reader is referred to Fox-Kemper et al. (2008) for a thorough discussion. Notice, however, that the framework described in section 3 can be easily extended to include the submesoscale parameterization scheme described in Fox-Kemper and Ferrari (2008).

c. *Transition layer*

Boundary layer thickness h and tracer distributions exhibit subsynoptic and mesoscale heterogeneity (Pollard et al. 1996; Legg et al. 1998; Ferrari and Rudnick 2000; Weller 2003). An average over this heterogeneity results in a transition layer with diabatic mixing of large-scale tracer distributions at a rate intermediate between the large BL and small interior rates. We define the transition layer as the layer containing all isopycnals within an averaging area and time interval that are intermittently exposed to strong turbulent mixing. This can occur either by entrainment into the BL as a result of mesoscale and internal wave heaving (i.e., vertical isopycnal displacements) or by other processes, such as subsynoptic surface fluxes, which induce subgrid-scale changes in h relative to isopycnal surfaces. The bottom of the transition layer is often characterized by large stratification and vertical tracer gradients generated through turbulent BL entrainment. Strong stratification plays an important role in parameterization schemes for microscale turbulent fluxes (Price et al. 1986; Large at al. 1994; Large et al. 1997) in relation to the rate that tracer and momentum anomalies pass between the BL and the mostly geostrophic interior flow.

From a mesoscale parameterization perspective, the transition layer represents the region that connects the adiabatic, eddy-induced, and tracer mixing in the stratified interior with the boundary-parallel, diapycnal fluxes in the BL. The thickness of the transition layer D is not well known yet, and analyses of relevant measurements and eddy-resolving computations are needed to provide better guidance. We present some preliminary scaling analysis to estimate D.

The magnitude of D is set both by subsynoptic and mesoscale fluctuations of h. The first contribution is the range of instantaneous h values around its time- and area-averaged value as diagnosed from a microscale BL parameterization applied locally. Danabasoglu et al. (2008) find that the base of the mixed layer tracks well the deepest values reached by the BL in the recent past. Hence, the difference between BL and mixed layer depth is a useful proxy for the synoptic contribution to D. Johnston and Rudnick (2007, submitted to *J. Phys. Oceanogr.*), using CTD and ADCP data, find that the base of the transition layer owing to subsynoptic variability is typically 10% deeper than the mixed layer depth because turbulent mixing partly penetrates into the stratified layer below the BL. This difference can be safely ignored at the level of approximation implicit in mesoscale parameterizations.

The second contribution to D is due to eddy heaving. A fluid parcel within a mesoscale eddy undergoes a vertical displacement ξ_e as it is adiabatically advected along a tilted isopycnal surface; hence $\xi_e \approx b_e/\partial_z b_m$ when $\partial_z b_e$ is neglected in the denominator. As a result, particles within a distance ξ_e from the BL base are episodically lifted into the BL and experience diabatic mixing. An estimate of the heaving contribution to the transition layer is the set of vertical levels z for which the root-mean-square ξ_e is larger than the distance from the BL base h,

$$\xi_{\mathrm{rms}} \equiv \sqrt{\langle \xi_e^2 \rangle} \approx \frac{\sqrt{\langle b_e^2 \rangle}}{\partial_z b_m} \geq |z + h|. \tag{11}$$

Kuo et al. (2005) computed the transition layer due to eddy heaving in a high resolution simulation of an oceanic jet configured to mimic the Antarctic Circumpolar Current system. The model was run without a BL scheme, and no mixed layer developed at the oceanic surface. Despite the lack of a surface BL, eddy fluxes had a diabatic component within a transition layer including all levels for which ξ_{rms} was larger than the distance from the surface. This simulation confirms that the diabatic component of the mesoscale eddy fluxes is not confined to the mixed layer, contrary to what is assumed in Treguier et al. (1997) and Griffies (2004). Diabatic fluxes develop wherever isopycnals outcrop at the surface in response to surface boundary conditions, regardless of whether there is a homogenized surface mixed layer.

Fluctuations of BL depth on synoptic time scales are well documented in the literature (e.g., Davis et al. 1981a,b). Here we use a combination of climatology and satellite data to estimate the eddy heaving contribution to the transition layer as defined in (11). The *World Ocean Atlas* climatology (Conkright et al. 1998) is used to compute $\partial_z b_m$. Buoyancy fluctuations b_e are estimated from altimetric measurements, assuming equipartition between eddy kinetic and available potential energies (Larichev and Held 1995; Eden 2007), so that

$$\xi_{\mathrm{rms}} = \sqrt{\frac{\langle b_e^2 \rangle}{(\partial_z b_m)^2}} \approx \sqrt{\frac{\langle |\mathbf{u}_e|^2 \rangle}{\partial_z b_m}}. \tag{12}$$

The near-surface eddy kinetic energy per unit mass on a global scale is computed from altimetric observations of sea level anomalies through the thermal wind relationship (Stammer 1997). The sea level data used are from the final combined processing of the Ocean Topography Experiment (TOPEX)/Poseidon and *European Remote Sensing Satellite* (*ERS*)*-1/2*. Anomalies are computed over a 5-yr time interval (October 1992–October 1997). Details of the calculation are given in Le Traon et al. (1998). Wunsch (1997) confirmed that altimetric estimates capture the bulk of the eddy kinetic energy associated with mesoscale eddies in low baroclinic modes needed for our calculation.

In Fig. 5a we show the transition layer depth estimated as the set of isopycnals that are occasionally entrained in the surface mixed layer according to (12). The mixed layer base is defined as the depth where potential density is 0.1 kg m^{-3} larger than the surface value (Fig. 5b). The calculation is done in terms of ML depth instead of BL depth because there are no global estimates of BL thickness. The transition layer is most significant in regions of enhanced eddy activity, like the Antarctic Circumpolar Current and western boundary currents where it can be as deep as the mixed layer depth. This estimate is likely to be an upper bound on D because ξ_{rms} is calculated using annually averaged vertical stratification. Annual averages tend to smooth out the strong stratification that often develops at the BL base and result in an overestimate of D.

Equation (11) can be used to derive an estimate of transition layer thickness in terms of mean climatological variables that are available in coarse resolution models. Following Large et al. (1997) we express the buoyancy fluctuations b_e as the product of a horizontal eddy mixing length R times the mean horizontal density gradient $|\nabla_{\mathrm{hor}} b_m|$. This scaling is supported by altimetric observations with the eddy mixing length given by the first baroclinic Rossby deformation radius (Stammer 1997),

$$R \approx \frac{1}{\pi |f|} \left[\int_{-H}^{\eta} (\partial_z b_m)^{1/2}\, \mathrm{d}z \right], \tag{13}$$

with H the oceanic depth and η the free surface elevation. Within a few degrees of the equator, (13) must be replaced by the equatorial deformation radius as dis-

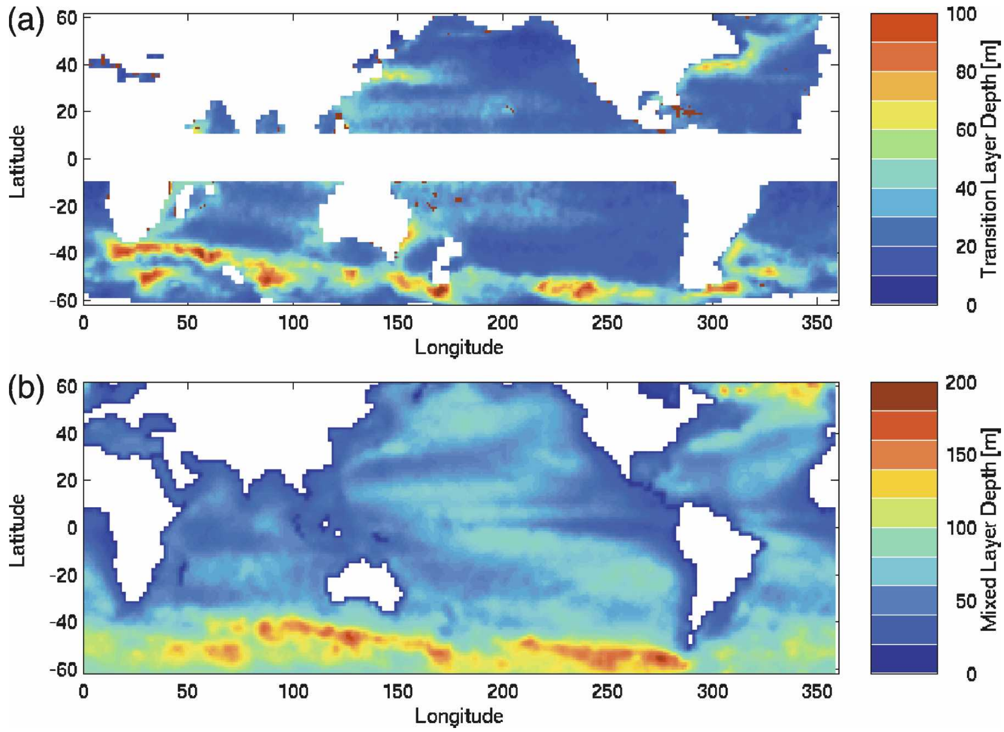

FIG. 5. (a) Transition layer depth estimated as the ratio of the altimetric eddy kinetic energy and the climatological stratification at the mixed layer base, see (11) (TOPEX/Poseidon data); (b) mixed layer depth defined as the depth where potential density is 0.1 kg m^{-3} larger than the surface value (*World Ocean Atlas*).

cussed in Griffies (2004). Under these approximations (11) becomes

$$\xi_{\rm rms} \approx \frac{|\nabla_{\rm hor} b_m|}{\partial_z b_m} R \geq |z + h|. \tag{14}$$

This expression further captures some of the synoptic variability of BL depth because it includes any mixed layer below the BL where $\partial_z b_m \approx 0$. Mixed layers deeper than the BL are part of the transition layer. They are a signature of regions where deep mixing took place in the past but is no longer active.

Now that we have an operational definition for the depth of the transition layer, we can proceed to derive guiding principles to parameterize the transition from diabatic to adiabatic eddy transport. In the transition layer the mean stratification is not necessarily zero, and mean buoyancy gradients can change in the vertical. However, eddy statistics transition smoothly between the interior and BL values (Cessi et al. 2006; Kuo et al. 2005). From a parameterization perspective this suggests that the full diffusivity tensor $\mathcal{K}$ that relates mesoscale fluxes and mean gradients must change smoothly though the transition layer,

$$\langle \mathbf{u}_e b_e \rangle = -\mathcal{K} \nabla b_m. \tag{15}$$

Using the decomposition in (9) and (10), the diffusivity tensor is composed of three terms: a symmetric term representing lateral diffusion across isopycnals,

$$\frac{\mathbf{F}_e\{b\} \cdot \nabla b_m}{|\nabla_{\rm hor} b_m|^2} = \frac{\langle \mathbf{u}_e b_e \rangle \cdot \nabla b_m}{|\nabla_{\rm hor} b_m|^2}, \tag{16}$$

and two antisymmetric terms representing the eddy-induced overturning streamfunctions in the x–z and y–z planes,

$$\boldsymbol{\Psi} \times \mathbf{z} = -\frac{\langle w_e b_e \rangle}{|\nabla_{\rm hor} b_m|^2} \nabla_{\rm hor} b_m. \tag{17}$$

The eddy-induced overturning streamfunction in the x–y plane $\boldsymbol{\Psi} \cdot \mathbf{z}$ is set to zero as required by continuity with the interior. Continuity of the diffusivity tensor then implies that both (16) and (17) are continuous within the transition layer and merge smoothly at the boundary and transition layer bases. Given continuity of the buoyancy field and its derivatives, this implies continuity of the fluxes.

3. Mesoscale eddy parameterization

We can now proceed to develop parameterizations for the eddy-induced velocity and the residual tracer fluxes applying the formalism developed in section 2.

a. Oceanic interior

In most OGCMs mesoscale fluxes in the interior are computed according to the parameterization first proposed by GM; that is, the fluxes are prescribed to be along mean density surfaces with the horizontal component satisfying a downgradient closure,

$$\langle \mathbf{u}_{he} b_e \rangle = -\kappa_{\rm GM} \boldsymbol{\nabla}_{\rm hor} b_m, \quad \langle w_e b_e \rangle = \kappa_{\rm GM} \frac{|\boldsymbol{\nabla}_{\rm hor} b_m|^2}{\partial_z b_m}. \tag{18}$$

Substituting these flux forms in the expressions for the eddy-induced streamfunction and residual flux into (5) and (7), or equivalently (9) and (10), yields

$$\boldsymbol{\Psi}_I = -\kappa_{\rm GM} \frac{\mathbf{z} \times \boldsymbol{\nabla}_{\rm hor} b_m}{\partial_z b_m}, \quad \mathbf{F}_e\{b\} = 0. \tag{19}$$

This form is the small-isopycnal-slope approximation in z coordinates for the thickness flux parameterization in isopycnal coordinates originally proposed by GM. This parameterization causes depletion of mean available potential energy (e.g., as in local baroclinic instability) and, implicitly, vertical diffusion of mean horizontal momentum (e.g., as in isopycnal form stress for a geostrophic flow). The horizontal diffusivity can be set either to a constant throughout the whole ocean or, following OGCM modeling practices after Smagorinsky (1963), it can be made flow dependent (Visbeck et al. 1997; Killworth 1997; Large at al. 2001; Smith and McWilliams 2003; Smith and Gent 2004).

The parameterization for the residual fluxes of tracers other than buoyancy is represented through additional isotropic diffusion along isopycnals as first suggested by Solomon (1971) and Redi (1982),

$$\mathbf{F}_e\{c\} = \kappa_{\rm GM} \left(\frac{\boldsymbol{\nabla} c_m \times \boldsymbol{\nabla} b_m}{|\boldsymbol{\nabla} b_m|^2} \right) \times \boldsymbol{\nabla} b_m. \tag{20}$$

We assume that the along-isopycnal diffusivity is equivalent to the GM diffusivity because other choices would lead to different mixing rates of buoyancy and tracers along the boundaries. CPH compare diffusivities estimated from passive and active tracers in the upper layers of an ocean simulation and do not find substantial differences. However, our expressions can be generalized to allow for different along-isopycnal and GM diffusivities if future studies suggest that they are indeed different.

The parameterization form in (20) is often replaced by its small-slope approximation, which is numerically more stable and less expensive (Griffies 2004),

$$\mathbf{F}_e\{c\} = -\kappa_{\rm GM}[\boldsymbol{\nabla}_{\rm hor} c_m + \partial_z c_m \mathbf{S}] - \kappa_{\rm GM}[|\mathbf{S}|^2 \partial_z c_m + \mathbf{S} \cdot \boldsymbol{\nabla}_{\rm hor} c_m]\mathbf{z}. \tag{21}$$

Here $\mathbf{S} = -\boldsymbol{\nabla}_{\rm hor} b_m / \partial_z b_m$ is the isopycnal slope vector. We will use the small-slope approximation throughout the paper, although all expressions can be extended to finite slopes.

Ferreira et al. (2005) recently proposed parameterizing eddies in models written in a transformed Eulerian mean formulation. In this formulation mesoscale eddies contribute as a stress $\tau_{\rm eddy}$ in the mean momentum equation given by

$$\boldsymbol{\tau}_{\rm eddy} = f \boldsymbol{\Psi}_I, \tag{22}$$

and through the residual fluxes $\mathbf{F}_e\{b\}$ and $\mathbf{F}_e\{c\}$ in the buoyancy and tracer equations. From our perspective any of GM, Ferreira et al. (2005), or some other parameterization for (7) are equivalent. Our purpose is to specify how the interior prescriptions for $\boldsymbol{\Psi}_I$, $\mathbf{F}_e\{b\}$, and $\mathbf{F}_e\{c\}$ should be modified near the boundaries.

b. Boundary and transition layers

In section 2 we argue that the symmetric and antisymmetric components of the mesoscale diffusivity tensor make a smooth transition from the interior to the surface values. We now derive a parameterization scheme consistent with these arguments.

The horizontal eddy fluxes are down the mean buoyancy gradient in the oceanic interior, representing the tendency of mesoscale eddies to reduce lateral buoyancy gradients and release available potential energy. Consistent with the argument that eddy statistics are continuous throughout the boundary and transition layers (section 2), we require that the horizontal eddy flux $\langle \mathbf{u}_{he} b_e \rangle$ remains down the horizontal buoyancy gradient, as in (18), with a continuous eddy diffusivity $\kappa_{\rm GM}$. The vertical component of the mesoscale eddy flux $\langle w_e b_e \rangle$ cannot be given by (18) because the vertical flux decreases to zero toward the surface, both to satisfy the no-normal-flow boundary condition and because the isopycnal eddy displacements b_e are reduced by the gravitational stiffness of the air–sea interface. In the BL we expect $\langle w_e b_e \rangle$ to be linear in z and $\boldsymbol{\nabla}_{\rm hor} b_m$ to be independent of z because strong mixing erases vertical gradients in both the horizontal mesoscale velocities and in the mean buoyancy gradients (section 2). A form for the vertical flux that satisfies these requirements and gives a continuous and differentiable eddy-induced streamfunction $\boldsymbol{\Psi}$ is

$$\frac{\langle w_e b_e \rangle}{|\boldsymbol{\nabla}_{\rm hor} b_m|^2} = -\frac{z - \eta}{h + \eta} \frac{\langle w_e b_e \rangle}{|\boldsymbol{\nabla}_{\rm hor} b_m|^2} \bigg|_{z=-h} \quad \text{for} \quad -h < z \leq \eta. \tag{23}$$

The subscript $z = -h$ indicates that the vertical flux and horizontal gradients are evaluated at the BL base

($z = -h$). The h in (23) is the large-scale boundary layer thickness averaged in time over any rapid BL fluctuations during which the eddy field is unlikely to change much, say a week. The time averaging is necessary because eddies respond only to low-frequency variations in BL depth, not to sudden deepening pulses or the diurnal cycle.

An arguably simpler choice is to set $\langle w_e b_e \rangle$ to be a linear function of z and neglect the $|\boldsymbol{\nabla}_{\rm hor} b_m|^2$ terms in (23). However, the resulting expression gives a nondifferentiable eddy-induced streamfunction and infinite eddy-induced velocities whenever $\boldsymbol{\nabla}_{\rm hor} b_m$ vanishes. This can be checked by substituting (23) into the expression for the eddy-induced streamfunction in (9).

The vertical fluxes in the transition layer are not linear in z because mixing is active only intermittently and shears can develop through geostrophic adjustment. Continuity of the eddy statistics requires that $\boldsymbol{\Psi}$ is continuous across the BL and transition layer boundaries. The simplest choice that allows for shear and has enough degrees of freedom to satisfy continuity of $\boldsymbol{\Psi}$, and its vertical derivative is

$$\frac{\langle w_e b_e \rangle}{|\boldsymbol{\nabla}_{\rm hor} b_m|^2} = \frac{(z+h)^2}{D^2}\left(-\frac{h+D+\eta}{h+\eta}\frac{\langle w_e b_e \rangle}{|\boldsymbol{\nabla}_{\rm hor} b_m|^2}\bigg|_{z=-h} + \frac{\langle w_e b_e \rangle}{|\boldsymbol{\nabla}_{\rm hor} b_m|^2}\bigg|_{z=-h-D}\right) - \frac{z-\eta}{h+\eta}\frac{\langle w_e b_e \rangle}{|\boldsymbol{\nabla}_{\rm hor} b_m|^2}\bigg|_{z=-h}, \quad \text{for} \quad -h-D < z \le -h. \tag{24}$$

The transition layer thickness D is estimated with the algorithm described in section 2c. The subscript $z = -h - D$ indicates that the vertical flux and horizontal gradients are evaluated at the base of the transition layer ($z = -h - D$). The expressions for the vertical eddy fluxes in (23) and (24) are continuous both at the BL base and at the transition layer base. The choice of imposing continuity of $\langle w_e b_e \rangle/|\boldsymbol{\nabla}_{\rm hor} b_m|^2$ instead of $\langle w_e b_e \rangle$ guarantees that $\boldsymbol{\Psi}$ remains continuous even where $\boldsymbol{\nabla}_{\rm hor} b_m$ vanishes.

We now have analytical expressions for the mesoscale fluxes in the boundary and transition layers. To complete the parameterization, we must constrain the remaining two free parameters: the vertical fluxes at the boundary and transition layer bases in (23) and (24). This is done by requiring that the vertical derivative of the eddy transport, $\partial_z \boldsymbol{\Psi}$, is continuous at the bases of the boundary and transition layers. Substituting these flux forms in the expressions for the eddy-induced streamfunction in (9) gives

$$\boldsymbol{\Psi} = -\kappa_{\rm GM} G(z)\mathbf{z} \times \frac{\boldsymbol{\nabla}_{\rm hor} b_m}{\partial_z b_m|_{z=-h-D}}, \tag{25}$$

where the vertical structure function $G(z)$ is defined by

$$G(z) = \begin{cases} -\dfrac{z-\eta}{2(h+\eta)+D}\left(2+\dfrac{D}{\lambda}\right), & \text{for} \quad -h < z \le \eta \text{ (BL)} \\ -\dfrac{(z+h)^2}{(h+D+\eta)^2-(h+\eta)^2}\left(1+\dfrac{D+h+\eta}{\lambda}\right) - \dfrac{z-\eta}{2(h+\eta)+D}\left(2+\dfrac{D}{\lambda}\right), & \text{for} \quad -h-D < z \le -h \\ & \text{(transition layer).} \end{cases} \tag{26}$$

The function $G(z)$ guarantees continuity and differentiability through the boundary and transition layers. At the base of the transition layer $G = 1$ and $\partial_z G = 1/\lambda$, where λ is a characteristic vertical length scale for the eddy fluxes below the transition layer, defined by

$$\lambda \equiv -\partial_z b_m / \partial_{zz} b_m|_{z=-h-D}.$$

Using the relationship between $\boldsymbol{\Psi}$ and $\langle w_e b_e \rangle$ in (17), the expression in (25) can be used to write final expressions for the fluxes in the transition and boundary layer,

$$\langle \mathbf{u}_{he} b_e \rangle = -\kappa_{\rm GM} \boldsymbol{\nabla}_{\rm hor} b_m,$$

$$\langle w_e b_e \rangle = \kappa_{\rm GM} G(z) \frac{|\boldsymbol{\nabla}_{\rm hor} b_m|^2}{\partial_z b_m|_{z=-h-D}}. \tag{27}$$

Substituting the expressions for buoyancy fluxes in the definition of the residual flux (10) gives

$$\mathbf{F}_b\{b\} = -\kappa_{\rm GM}\left[1 - G(z)\frac{\partial_z b_m}{\partial_z b_m|_{z=-h-D}}\right]\boldsymbol{\nabla}_{\rm hor} b_m. \tag{28}$$

The derivation of the expression for the residual tracer flux is sketched in appendix B and is

$$\mathbf{F}_b\{c\} = -\kappa_{\mathrm{GM}}\left[\boldsymbol{\nabla}_{\mathrm{hor}}c_m - G(z)\frac{\partial_z c_m}{\partial_z b_m|_{z=-h-D}}\boldsymbol{\nabla}_{\mathrm{hor}}b_m\right] - \kappa_{\mathrm{GM}}G(z)\left(\frac{|\boldsymbol{\nabla}_{\mathrm{hor}}b_m|^2}{\partial_z b_m|_{z=-h-D}}\frac{\partial_z c_m}{\partial_z b_m} - \frac{\boldsymbol{\nabla}_{\mathrm{hor}}b_m\cdot\boldsymbol{\nabla}_{\mathrm{hor}}c_m}{\partial_z b_m|_{z=-h-D}}\right)\mathbf{z}. \quad (29)$$

This expression matches the small-slope Redi tensor in the ocean interior and it reduces to (28) when $b = c$. The formula can be generalized to match the finite slope Redi tensor in the interior, but we stick to common practice and report only the small slope expressions. Notice that the small slope approximation is made only in the adiabatic interior. No such assumption is made in the boundary and transition layers where slopes can, and usually do, become large.

Equations (25), (28), and (29) constitute the full parameterization scheme in the boundary and transition layers. These equations follow from the eddy flux decomposition in (9) and (10) under the assumptions that the horizontal eddy fluxes of all tracers are down their local mean horizontal gradients and the vertical eddy fluxes decrease to zero within the boundary and transition layers. The decrease is linear in the BL and quadratic in the transition layer. These simple requirements give a parameterization scheme that ensures the following properties:

1) The residual velocities and residual fluxes vanish at the oceanic boundaries.
2) The residual streamfunction and the residual velocities are continuous everywhere.
3) The residual circulation releases available potential energy everywhere.
4) The shear in the residual velocities acts to restratify the water column through the transition layer but not within the boundary layer (as long as buoyancy is well mixed through the mixed layer).
5) The residual fluxes and their divergence are continuous if the b_m and c_m gradients are continuous.

The first property is imposed through the vertical structure functions $G(z)$ and $G'(z)$, which vanish at the boundaries. The second property follows from the continuity of $\boldsymbol{\Psi}_z$. The third property is guaranteed by having the residual streamfunction in the direction of the local horizontal buoyancy gradient so that the release of available potential energy is nonnegative definite everywhere; that is, $\langle w_e b_e\rangle = \boldsymbol{\Psi} \times \boldsymbol{\nabla}_{\mathrm{hor}}b_m \cdot \mathbf{z} \geq 0$. The fourth property is consistent with the observation that vertical mixing erases mesoscale shears in the BL so that any shear in the horizontal eddy-induced velocity is confined below the BL in the transition layer and in the oceanic interior. The fifth property guarantees that the eddy forcing in the tracer equations does not produce singularities starting from smooth tracer distributions.

c. *Boundary and transition layers: Alternative expressions*

Treguier et al. (1997) suggested that parameterization of eddy fluxes at the oceanic boundaries should include along-boundary eddy-induced velocity and residual flux of buoyancy. We further argue that the eddy-induced velocity should be continuous in z with zero shear in the BL and with a constant shear in the transition layer. There are many parameterization forms that can satisfy these requirements. One such form—our preference—is derived in section 3b and results in the expressions (25) and (28). Alternative forms have been recently proposed in the literature. We wish to compare our approach to these alternative schemes.

Danabasoglu et al. (2008) assume that the eddy-induced streamfunction is set at the base of the transition layer and decays to zero quadratically in the transition layer and linearly in the BL. Continuity of the eddy-induced velocity is imposed at the transition and boundary layer bases. These simple rules fully determine $\boldsymbol{\Psi}$:

$$\boldsymbol{\Psi} = \kappa_{\mathrm{GM}}G_1(z)\mathbf{z}\times\left.\frac{\boldsymbol{\nabla}_{\mathrm{hor}}b_m}{\partial_z b_m}\right|_{z=-h-D} + \kappa_{\mathrm{GM}}G_2(z)\mathbf{z}\times\left.\frac{\partial}{\partial z}\frac{\boldsymbol{\nabla}_{\mathrm{hor}}b_m}{\partial_z b_m}\right|_{z=-h-D}, \quad (30)$$

where the vertical structure functions that guarantee continuity are

$$G_1(z) = \begin{cases} \dfrac{2(z-\eta)}{2(h+\eta)+D}, & \text{for} \quad -h < z \leq \eta \text{ (BL)} \\ \dfrac{(z+h)^2}{(h+D+\eta)^2-(h+\eta)^2} + \dfrac{2(z-\eta)}{2(h+\eta)+D}, & \text{for} \quad -h-D < z \leq -h \text{ (transition layer)}, \end{cases}$$

$$G_2(z) = \begin{cases} \dfrac{D(z-\eta)}{2(h+\eta)+D}, & \text{for} \quad -h < z \leq \eta \text{ (BL)} \\ \dfrac{(z+h)^2(D+h+\eta)}{(h+D+\eta)^2-(h+\eta)^2} + \dfrac{D(z-\eta)}{2(h+\eta)+D}, & \text{for} \quad -h-D < z \leq -h \text{ (transition layer)}. \end{cases}$$

The main difference between this approach and the one proposed in section 3b is that the direction of $\boldsymbol{\Psi}$ is here set by the buoyancy gradients at the transition layer base instead of being set by the local buoyancy gradient as in (9). The implication is that in this formulation $\boldsymbol{\Psi}$ is not guaranteed to reduce the mean potential energy; that is, $\langle w_e b_e \rangle = \boldsymbol{\Psi} \times \boldsymbol{\nabla}_{\rm hor} b_m \cdot \mathbf{z}$ is not sign definite. However, this expression reduces to (9) if the direction of the horizontal buoyancy gradients does not veer much in the transition and boundary layers.

Danabasoglu et al. (2008) assume that the diabatic residual buoyancy flux grows linearly from zero in the interior to along boundary in the BL, that is,

$$\mathbf{F}_e\{b\} = -\kappa_{\rm GM}[\boldsymbol{\nabla}_{\rm hor} b_m - G_3(z)\boldsymbol{\nabla}_{\rm hor} b_m],$$
$$\mathbf{F}_e\{c\} = -\kappa_{\rm GM}[\boldsymbol{\nabla}_{\rm hor} c_m - G_3(z)\mathbf{S}\partial_z c_m] + \kappa_{\rm GM} G_3(z)(|\mathbf{S}|^2 \partial_z c_m + \mathbf{S}\cdot\boldsymbol{\nabla}_{\rm hor} c_m)\mathbf{z}, \tag{31}$$

where

$$G_3(z) = \begin{cases} 0, & \text{for} \quad -h < z \le \eta \text{ (BL)} \\ \dfrac{(z+h)}{D}, & \text{for} \quad -h - D < z \le -h \text{ (transition layer).} \end{cases}$$

In the BL this approach gives the approximately same residual buoyancy flux as (28) because $\partial_z b_m \approx 0$, while the residual tracer flux differs by the vertical component. In the transition layer the details of the vertical structure of the residual fluxes are also different. Furthermore, (31) does not guarantee continuity of the vertical flux divergence at the transition layer base. Despite these differences, the two expressions are likely to be quite similar in most situations, because they both capture the transition from along-isopycnal residual fluxes in the interior to along-boundary fluxes in the BL with some degree of smoothness.

The parameterization forms in (30) and (31) reduce to those of Griffies (2004) in the limit of vanishing transition layer thickness D. A zero D has the effect of introducing discontinuities in the eddy-induced velocities, and it is not consistent with high-resolution numerical results (Kuo et al. 2005). In the next section we discuss why such discontinuities are undesirable and can lead to spurious numerical instabilities. In summary we believe that the expressions in (25), (28), and (29) constitute a superior parameterization scheme with a number of desirable properties, but the forms in (30) and (31) may often produce similar results in practice.

4. Numerical experiment

Our ideas about eddy parameterizations at the oceanic boundaries are now illustrated through a simple numerical experiment. We study the spreading of a warm lens that outcrops in a mixed layer at the oceanic surface and lies on top of a stratified ocean, as shown in Fig. 6a.

The geometry, forcing, and boundary conditions do not depend on the zonal direction x. Thus we can solve for the zonally averaged circulation in the form

$$\overline{\mathbf{u}}_t + \overline{\mathbf{u}}\cdot\boldsymbol{\nabla}\overline{\mathbf{u}} + f\mathbf{z}\times\overline{\mathbf{u}} = -\boldsymbol{\nabla}\overline{p} - \boldsymbol{\nabla}\mathbf{F}_e\{\mathbf{u}\} + \boldsymbol{\nabla}\cdot(\nu\boldsymbol{\nabla}\overline{\mathbf{u}}), \tag{32}$$

$$0 = -\overline{p}_z + \overline{b}, \tag{33}$$

$$\overline{v}_y + \overline{w}_z = 0, \tag{34}$$

$$\overline{b}_t + (\overline{\mathbf{u}} + \overline{\mathbf{u}}_{me})\cdot\boldsymbol{\nabla}\overline{b} = -\boldsymbol{\nabla}\cdot\mathbf{F}_e\{b\} + \boldsymbol{\nabla}\cdot(\kappa\boldsymbol{\nabla}\overline{b}) + \overline{\mathcal{B}}_z. \tag{35}$$

The overbar here denotes the zonal average over the domain length L_x:

$$\overline{b} = \frac{1}{L_x}\int_0^{L_x} b(x, y, z, t)\,\mathrm{d}x. \tag{36}$$

The surface buoyancy flux is represented by $\mathcal{B}$. We impose a rigid upper lid at $z = 0$ and a flat bottom at $z = -H$ and use periodic boundary conditions in x. The zonally averaged equations are solved with the MIT OGCM (Marshall et al. 1997).

The model ocean is 2000 km wide and 2000 m deep with a flat bottom (Table 1). The horizontal resolution is 100 km, while the vertical resolution is variable: 20 m in the upper 200 m, increasing exponentially with depth with a stretching scale of 1.2. Boundary conditions are periodic on the lateral walls. Heat satisfies the zero flux boundary conditions at the surface and bottom. For momentum we use no slip at the bottom and free slip at the surface. The parameters used in the simulation are listed in Table 1. At this resolution mesoscale and microscale processes are subgrid scale and must be parameterized.

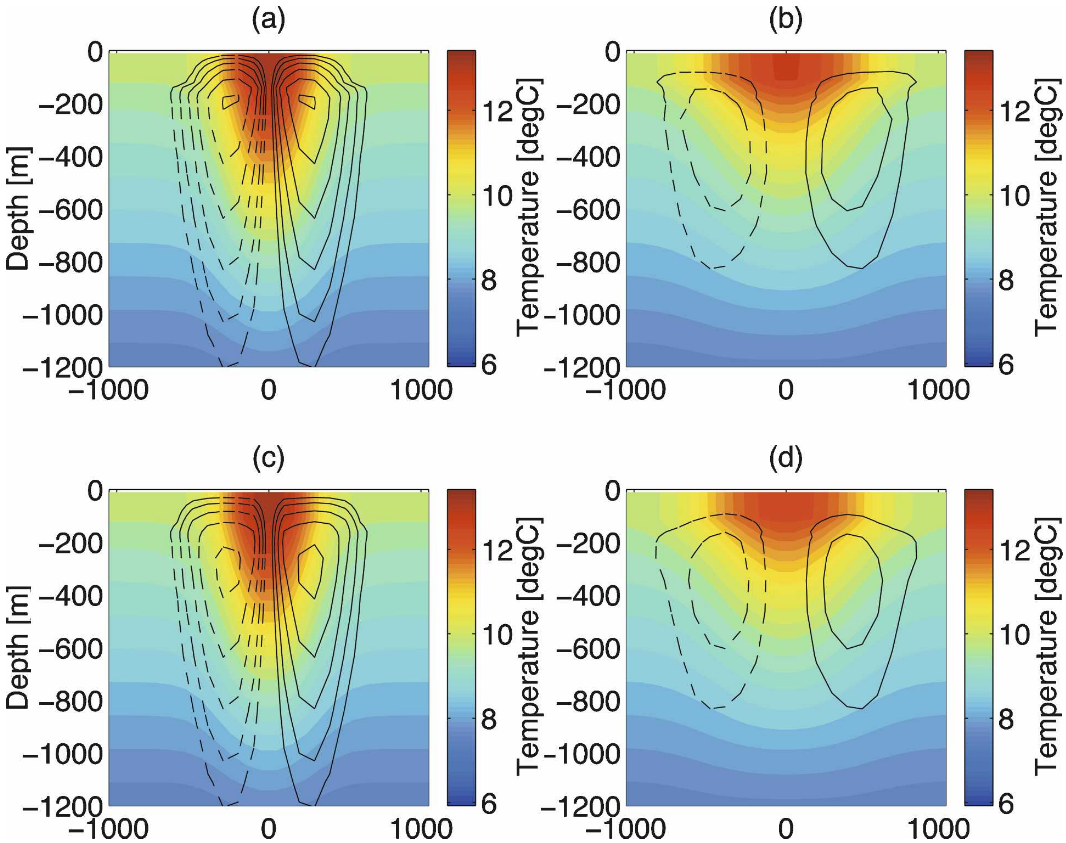

FIG. 6. Evolution of a warm lens on top of a stably stratified ocean: (left) the initial condition and (right) the solution after one year. There is a boundary layer in the upper 140 m. The color contours represent temperature and the lines represent the eddy-induced circulation: full lines for clockwise rotation and dashed lines for anticlockwise rotation. (top) Solutions using the parameterization scheme described in (9) and (10) with the transition layer thickness estimated according to (11) and (bottom) solutions obtained using the same parameterization, but a transition layer 10 times thicker.

The microscale fluxes are parameterized as downgradient fluxes of momentum and buoyancy: in the interior the microscale viscosity is set to $\nu = 2 \times 10^{-4}$ m^2 s^{-1} and the microscale diffusivity to $\kappa = 2 \times 10^{-5}$ m^2 s^{-1}. A BL is represented in the upper 140 m by increasing the microscale viscosity and diffusivity to 1×10^{-3} m^2 s^{-1}. Convective adjustment is used to remove unstable stratification.

TABLE 1. Parameters used in the spreading warm lens experiment.

Boundary layer depth	h	140 m
Oceanic depth	H	2000 m
Vertical diffusivity in the boundary layer	κ_{BL}	10^{-3} m^2 s^{-1}
Vertical viscosity in the boundary layer	ν_{BL}	10^{-3} m^2 s^{-1}
Vertical diffusivity in the interior	κ	2×10^{-5} m^2 s^{-1}
Vertical viscosity in the interior	ν	2×10^{-4} m^2 s^{-1}
Horizontal viscosity	A	2×10^{5} m^2 s^{-1}
Eddy diffusivity	κ_{GM}	1000 m^2 s^{-1}

The horizontal components of the mesoscale Reynolds stress tensor are parameterized with a horizontal viscosity in the horizontal momentum equation $\mathbf{F}_e\{\mathbf{u}\} = -A\,\nabla_{hor}\mathbf{u}_{hor}$, with $A = 2 \times 10^5$ m^2 s^{-1}. The mesoscale buoyancy fluxes are parameterized as an eddy-induced velocity $\bar{\mathbf{u}}_{me} = \nabla \times \mathbf{\Psi}$ and a diffusive flux $\mathbf{F}_e\{b\}$. In the oceanic interior we use the GM scheme for $\mathbf{\Psi}$ in (19) with a diffusivity κ_{GM} of 1000 m^2 s^{-1}. The residual buoyancy flux $\mathbf{F}_e\{b\}$ is set to zero under the assumption that eddy fluxes are adiabatic. In the transition and boundary layers, $\mathbf{\Psi}$ and $\mathbf{F}_e\{b\}$ are computed from the expressions in (25) and (28).

We start the simulations with a background stratification of $N = 1 \times 10^{-3}$ s^{-1}. The warm lens is represented as an anomaly with a maximum amplitude of 3.5°C at the surface, confined to the upper 600 m and with an horizontal extent of about 500 km. The zonal velocity field is initially in geostrophic balance, while the meridional and vertical velocities start from zero.

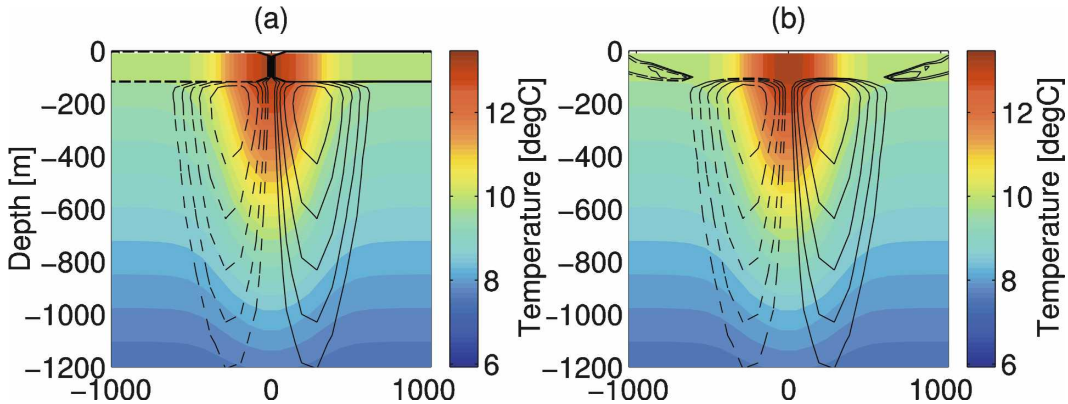

FIG. 7. The eddy-induced overturning circulation produced by two different parameterization schemes for the slumping of a warm lens on top of a stably stratified ocean for the same initial condition shown in Fig. 6: (left) the GM parameterization and (right) the GM parameterization with the tapering scheme suggested by Danabasoglu et al. (1994) to suppress spurious circulations in regions of weak stratification.

The initial geostrophic shear is chosen to be baroclinically unstable (i.e., in a high-resolution, three-dimensional simulation the lens would slump and shed baroclinic eddies). No eddies develop in our model because the grid is too coarse to resolve the wavenumbers at which the instability should develop. This is where the mesoscale parameterization comes in. The GM parameterization scheme mimics the effect of the unresolved eddy field and acts to flatten the mean isopycnals.

In Fig. 6 we show the stratification and the eddy-induced streamfunction produced by the GM parameterization scheme in the interior and the scheme in (25), (28), and (29) in the boundary and transition layers. The eddy-induced streamfunction has a smooth transition from the adiabatic interior to the BL without creating spurious shears in the BL. The lens spreads at a similar rate in the interior and in the upper ocean so that no discontinuities develop at the transition layer base. The temperature anomaly in the BL decreases with time as a result of the diapycnal horizontal eddy flux.

The thickness D of the transition zone plays an important role in the evolution of the lens. In Figs. 6a and 6b, we show solutions with D computed according to the formulas given in section 2c. For the parameters chosen in this example, $D \approx 30$ m. One can see a slight discontinuity in the eddy-induced circulation across the BL base. In Figs. 6c and 6d, we show a solution where we increased D by 10 times: as a result, the transition between the BL and the interior is more gradual. The guiding principles used to determine D are preliminary. Direct numerical simulations of an eddying field outcropping at the surface are necessary to settle this issue. The question of how D is determined is of crucial importance because the behavior of the eddy fluxes at the base of the BL can substantially modify the ventilation of the oceanic interior.

The parameterization proposed here differs in important aspects from parameterization described in the literature. Figure 7a shows the overturning circulation obtained by applying the GM parameterization throughout the whole water column. The overturning circulation acts to spread the lens laterally and reduce the available potential energy. The overturning is largest at the surface where the stratification is weak. However, the condition $\boldsymbol{\Psi} = 0$ at $z = 0$ forces the streamlines to close at the surface and generates two surface-intensified overturning cells. These cells create a large shear in the upper ocean and restratify the boundary layer despite strong vertical mixing. Both the surface overturning circulation and the strong restratification are physically implausible: there is no numerical or observational evidence for strong surface-trapped recirculations of this kind.

A common solution to avoid surface-intensified overturning cells in current OGCMs is to set $\boldsymbol{\Psi}$ to zero before reaching the BL through ad hoc tapering functions, as shown in Fig. 7b (Gerdes et al. 1991; Danabasoglu et al. 1994). This has the awkward consequence of creating a strong horizontal eddy-induced mass flux immediately below the BL and none within it (Large et al. 1997). Furthermore the tapering approach does not include any diabatic horizontal flux. As a result the lens spreading proceeds faster in the oceanic interior than at the surface because there is no parameterization of eddy transport in the boundary layer. What Gerdes et al. (1991) and Danabasoglu et al. (1994) failed to realize is that the restratification associated with the surface-trapped circulations can be eliminated by imposing that

$\boldsymbol{\Psi}$ has a linear gradient in z within the BL so that the eddy-induced velocity has zero shear. No spurious boundary layer restratification occurs in this case, but eddy transport is not artificially suppressed at the oceanic surface. Preliminary experiments with the MIT general circulation model show that these differences are significant and strongly support the approach described here (Ferrari 2006).

More recently, Griffies (2004) has proposed to taper $\boldsymbol{\Psi}$ linearly to zero using a scheme similar to the one presented here but without a transition layer. Without a transition layer, discontinuities in the eddy-induced velocity develop at the BL base (Fig. 4), and a convective adjustment scheme is necessary to prevent generation of unstable stratification (Griffies et al. 2005). The generation of convective instabilities by mesoscale motions has no physical justification and compromises the proper exchange of properties between the BL and the oceanic interior. In a sense the Griffies approach goes too far in suppressing the excessive GM restratification in regions of low stratification and ends up producing additional vertical mixing.

5. Conclusions

Mesoscale eddy transport of large-scale momentum and material tracers exerts a profound influence on the oceanic general circulation and on the exchange of heat, freshwater, and other material between the ocean and the atmosphere. The mesoscale parameterizations used in OGCMs typically represent the adiabatic release of potential energy by baroclinic instability in the interior, as suggested by GM. However, as the surface is approached, eddy fluxes develop a substantial diabatic component because density becomes vertically well mixed in the boundary layer (BL) while eddy and mean motions are kinematically constrained to be nearly parallel to the boundary (i.e., horizontal near the surface). As a result, quasi-adiabatic schemes lead to unphysical behaviors at the boundaries. Too often OGCM practice has been to taper the mesoscale eddy fluxes to vanish within the boundary layers. This is not physically correct. Mesoscale eddy fluxes play an important role in the tracer transport along the oceanic boundaries and must be parameterized in coarse resolution models. The solution proposed in this paper is to modify the interior parameterization to account for the different eddy fluxes in the BL with a smooth transition through a layer of subgrid-scale intermittent diabatic mixing.

A parameterization for the mesoscale eddy fluxes near the oceanic boundaries is derived starting from the physical argument that eddy fluxes are adiabatic in the interior, diabatic in the BLs, and zero in their normal component at the boundaries. We restrict the discussion to tracer fluxes, but our arguments are likely to be germane to momentum fluxes as well and could be applied to derive matching conditions for momentum fluxes at the ocean surface. We split the mesoscale tracer flux $\langle \mathbf{u}_e c_e \rangle$ into an advective component $\overline{\mathbf{u}}_{me} \cdot \boldsymbol{\nabla}\langle c \rangle$ and a residual component $\mathbf{F}_e\{c\}$, usually represented as a diffusion process. The constraint that there is no eddy flux in and out of the ocean can be translated into the conditions that the eddy-induced velocity $\overline{\mathbf{u}}_{me}$ and the diffusive flux $\boldsymbol{F}_e\{c\}$ are oriented parallel to the boundaries at the solid walls and at the free surface. Equations (25), (28), and (29) constitute the full parameterization scheme and satisfy the following properties:

1) In the interior we assume that an adiabatic parameterization scheme is known, be it the scheme of GM or a scheme based on residual eddy stress (Ferreira et al. 2005). This scheme is then used to derive expressions for $\mathbf{u}_{me}$ and $\mathbf{F}_e\{c\}$ away from the boundaries.
2) In the BLs we assume that $\overline{\mathbf{u}}_{me}$ has no vertical shear, as long as buoyancy is well mixed through the mixed layer, in the spirit of well-mixed BL models. The residual buoyancy flux is parameterized as a downgradient flux parallel to the boundaries; that is, there is a diapycnal eddy flux.
3) The interior and BL parameterizations are matched by quadratically interpolating the eddy fluxes through a transition layer of thickness D. The matching condition of continuous eddy-induced velocity and diffusive flux divergence at the boundary and transition layer bases are sufficient to derive expressions for $\overline{\mathbf{u}}_{me}$ and $\mathbf{F}_e\{c\}$ in the boundary layers. The transition layer represents the region through which the mesoscale eddy flux develops a diabatic component through intermittent BL mixing beneath the resolution scale of the mean circulation. Consistent with the idea of intermittent mixing, we allow for shear in $\overline{\mathbf{u}}_{me}$ so that restratification occurs in the transition layer. We propose a simple scaling argument to estimate D based on eddy heaving, but a more satisfactory parameterization of D will require high-resolution numerical simulations and careful field experiments.

The new parameterization scheme is illustrated by an idealized zonal flow that uses a GM parameterization scheme in the interior. The proposed BL parameterization represents a clear improvement over tapering schemes described in the literature. The new parameterization scheme does not to trigger any numerical instabilities in the low-stratification regions near the boundaries (unlike a recent parameterization proposed by Griffies 2004). It is quite possible that the boundary layer closure scheme can be applied to interior regions of low stratification as well, thus eliminating any need to introduce artificial tapering functions to maintain numerical stability.

Acknowledgments. This research was supported by NSF Grants OCE02-41528 (RF), CE02-21177 (JM), and OCE03-36755 (joint). The authors wish to thank J. Marshall and A. Plumb for many useful conversations and suggestions and G. Danabasoglu for advice about OGCM implementation of the parameterization. V. Canuto and M. Dubovikov were included as coauthors during the review process, because they contributed to resolving some inconsistencies in the original expressions for the eddy-induced streamfunction and the residual fluxes.

APPENDIX A

Definitions of $\boldsymbol{\Psi}$ and $\mathbf{F}_e\{b\}$ at Oceanic Boundaries

Eddy fluxes veer from along isopycnal to along boundary as the boundary is approached. To represent this transition, it is useful to modify the definition of $\boldsymbol{\Psi}$ in (4) so that the transition to no-normal boundary flow is achieved through a layer with finite thickness. The transition can be achieved by exploiting the arbitrariness in the choice of the vector streamfunction $\boldsymbol{\Psi}$ to define an eddy-induced velocity that satisfies no-normal flow boundary conditions. Following Treguier et al. (1997), we generalize the definition of $\boldsymbol{\Psi}$ to be

$$\boldsymbol{\Psi} \equiv -\frac{\langle \mathbf{u}_e b_e \rangle \times \nabla b_m}{|\nabla b_m|^2} - \frac{\langle \mathbf{u}_e b_e \rangle \cdot \nabla b_m}{|\nabla b_m|^2}\boldsymbol{\alpha}, \quad \text{(A1)}$$

where $\boldsymbol{\alpha}$ is an arbitrary three-dimensional vector that may be spatially and temporally variable. The residual buoyancy flux must be modified accordingly:

$$\mathbf{F}_e\{b\} \equiv \frac{\langle \mathbf{u}_e b_e \rangle \cdot \nabla b_m}{|\nabla b_m|^2}(\nabla b_m + \boldsymbol{\alpha} \times \nabla b_m). \quad \text{(A2)}$$

The residual flux remains proportional to the diapycnal flux in this generalized formulation, but it points in a direction that depends on the choice of $\boldsymbol{\alpha}$, not down the mean buoyancy gradient. The eddy-induced circulation remains largely unaltered in the oceanic interior where diapycnal fluxes are weak, but it is modified at the boundaries where eddy-driven diapycnal transports are large.

The vector $\boldsymbol{\alpha}$ can be chosen so that the component of the diapycnal flux that cancels the advection through the boundary is retained in the definition of $\boldsymbol{\Psi}$ so that the no-normal flow boundary condition is satisfied. Consider a boundary surface with unit normal, $\mathbf{n}$ A form for $\boldsymbol{\alpha}$ that satisfies this boundary conditions is

$$\boldsymbol{\alpha} \equiv \frac{\mathbf{n} \cdot \nabla b_m}{|\nabla b_m|^2 - |\mathbf{n} \cdot \nabla b_m|^2}\mathbf{n} \times \nabla b_m. \quad \text{(A3)}$$

The corresponding vector streamfunction is

$$\boldsymbol{\Psi} = -\frac{\langle \mathbf{u}_e b_e \rangle \cdot \mathbf{n}}{|\nabla b_m|^2 - |\mathbf{n} \cdot \nabla b_m|^2}\mathbf{n} \times \nabla b_m - \frac{(\langle \mathbf{u}_e b_e \rangle \times \nabla b_m) \cdot \mathbf{n}}{|\nabla b_m|^2 - |\mathbf{n} \cdot \nabla b_m|^2}\mathbf{n}. \quad \text{(A4)}$$

It has two components: the first represents a circulation directed across the boundaries that vanishes because the eddy velocity normal to the boundary is zero, and the second represents a circulation along the boundary.

The associated diabatic residual flux is directed parallel to the boundary:

$$\mathbf{F}_e\{b\} = \frac{\langle \mathbf{u}_e b_e \rangle \cdot \nabla b_m}{|\nabla b_m|^2 - |\mathbf{n} \cdot \nabla b_m|^2}[\nabla b_m - (\nabla b_m \cdot \mathbf{n})\mathbf{n}]. \quad \text{(A5)}$$

The definition in (A4) satisfies the no-normal flow condition $\mathbf{u}_{me} \cdot \mathbf{n} = 0$, and can be applied close to the boundaries.

The gauge invariance can now be used to define eddy-induced circulations and residual fluxes that vanish at all boundaries and retain useful forms in the interior. The choice of gauge in the interior is inconsequential because away from boundaries there is no buoyancy flux across isopycnals and the gauge terms in (A1) and (A2) vanish for any choice of $\boldsymbol{\alpha}$. Hence we can define $\boldsymbol{\alpha}$ as in (A3) where $\mathbf{n}$ is set to the vertical unit vector at the surface and smoothly transitions to the unit vector normal to topography toward the bottom. For a flat bottom ocean $\mathbf{n} = \mathbf{z}$ can be used everywhere; this choice might be appropriate even in the presence of topographic relief if eddy fluxes are weak at the ocean bottom.

APPENDIX B

Residual Fluxes of Passive Tracers

The decomposition of the eddy tracer flux into advective and residual components corresponding to (9) and (10) is

$$\langle \mathbf{u}_e c_e \rangle = \boldsymbol{\Psi} \times \nabla c_m + \mathbf{F}_e\{c\}, \quad \text{(B1)}$$

where $\boldsymbol{\Psi}$ is given in (9) and the residual flux is

$$\mathbf{F}_e\{c\} = \left(\frac{\langle w_e b_e\rangle}{|\boldsymbol{\nabla}_{\rm hor} b_m|^2}\mathbf{z}\times\boldsymbol{\nabla}_{\rm hor} b_m - \frac{\langle w_e c_e\rangle}{|\boldsymbol{\nabla}_{\rm hor} c_m|^2}\mathbf{z}\times\boldsymbol{\nabla}_{\rm hor} c_m\right)\times\boldsymbol{\nabla} c_m + \left(\frac{\langle \mathbf{u}_{he} b_e\rangle\times\boldsymbol{\nabla}_{\rm hor} b_m}{|\boldsymbol{\nabla}_{\rm hor} b_m|^2} - \frac{\langle \mathbf{u}_{he} c_e\rangle\times\boldsymbol{\nabla}_{\rm hor} c_m}{|\boldsymbol{\nabla}_{\rm hor} c_m|^2}\right)\times\boldsymbol{\nabla} c_m + \frac{\langle \mathbf{u}_e c_e\rangle\cdot\boldsymbol{\nabla} c_m}{|\boldsymbol{\nabla}_{\rm hor} c_m|^2}\boldsymbol{\nabla}_{\rm hor} c_m. \quad \text{(B2)}$$

We used a downgradient closure for the horizontal flux of buoyancy. It seems consistent to assume the same for the tracer flux, that is,

$$\langle \mathbf{u}_{he} c_e\rangle = -\kappa_{\rm GM}\boldsymbol{\nabla}_{\rm hor} c_m. \quad \text{(B3)}$$

Imposing the downgradient closures for the horizontal fluxes of buoyancy and tracer, the residual flux in (B2) becomes

$$\mathbf{F}_e\{c\} = -\kappa_{\rm GM}\boldsymbol{\nabla}_{\rm hor} c_m + \frac{\langle w_e b_e\rangle\partial_z c_m}{|\boldsymbol{\nabla}_{\rm hor} b_m|^2}\boldsymbol{\nabla}_{\rm hor} b_m + \left(\langle w_e c_e\rangle - \langle w_e b_e\rangle\frac{\boldsymbol{\nabla}_{\rm hor} b_m\cdot\boldsymbol{\nabla}_{\rm hor} c_m}{|\boldsymbol{\nabla}_{\rm hor} b_m|^2}\right)\mathbf{z}.$$

Imposing continuity of the vertical fluxes and their divergences at the boundary and transition layer interfaces gives the expression in (29). The expression involves division by the weak stratification in the mixed layer and might be problematic for numerical implementation. An alternative expression that satisfies the same properties, but avoids division by a weak stratification, is

$$\mathbf{F}_e\{c\} = -\kappa_{\rm GM}\left[\boldsymbol{\nabla}_{\rm hor} c_m - G(z)\frac{\partial_z c_m}{\partial_z b_m|_{z=-h-D}}\boldsymbol{\nabla}_{\rm hor} b_m\right] - \kappa_{\rm GM}\hat{G}(z)\left[\frac{|\boldsymbol{\nabla}_{\rm hor} b_m|^2}{\partial_z b_m|^2_{z=-h-D}}\partial_z c_m - \frac{\boldsymbol{\nabla}_{\rm hor} b_m\cdot\boldsymbol{\nabla}_{\rm hor} c_m}{\partial_z b_m|^2_{z=-h-D}}\partial_z b_m\right]\mathbf{z}.$$

The function $\hat{G}(z)$ has the same form of $G(z)$ in (26) except for the definition of λ. At the base of the transition layer $\hat{G} = 1$ and $\partial_z\hat{G} = 1/\lambda_2$, where $\lambda_2 = \lambda/2$. This alternative expression is not our favorite choice because it does not preserve the symmetric nature of the diffusivity tensor, but it might be advantageous to ensure numerical stability.

REFERENCES

Andrews, D. G., and M. E. McIntyre, 1978: Generalized Eliassen-Palm and Charney-Drazin theorems for waves on axisymmetric mean flows in compressible atmospheres. *J. Atmos. Sci.,* **35,** 175–185.

Boccaletti, G., R. Ferrari, and B. Fox-Kemper, 2007: Mixed layer instabilities and restratification. *J. Phys. Oceanogr.,* **37,** 2228–2250.

Cessi, P., W. R. Young, and J. A. Polton, 2006: Control of large-scale heat transport by small-scale mixing. *J. Phys. Oceanogr.,* **36,** 1877–1894.

Conkright, M., S. Levitus, T. O'Brien, T. Boyer, J. Antonov, and C. Stephens, 1998: World ocean atlas 1998 CD-ROM data set documentation. NODC Internal Rep., Tech. Rep. 15.

Danabasoglu, G., and J. C. McWilliams, 1995: Sensitivity of the global ocean circulation to parameterizations of mesoscale tracer transports. *J. Climate,* **8,** 2967–2987.

——, ——, and P. R. Gent, 1994: The role of mesoscale tracer transports in the global ocean circulation. *Science,* **264,** 1123–1126.

——, R. Ferrari, and J. C. McWilliams, 2008: Sensitivity of an ocean general circulation model to a parameterization of near-surface eddy fluxes. *J. Climate,* **21,** 1192–1208.

Davis, R. E., 1994: Diapycnal mixing in the ocean: The Osborn–Cox model. *J. Phys. Oceanogr.,* **24,** 2560–2576.

——, R. deSzoeke, D. Halpern, and P. Niiler, 1981a: Variability in the upper ocean during MILE. Part I: The heat and momentum balances. *Deep-Sea Res.,* **28A,** 1427–1451.

——, ——, ——, and ——, 1981b: Variability in the upper ocean during MILE. Part II: Modeling the mixed layer response. *Deep-Sea Res.,* **28A,** 1453–1475.

Drijfhout, S. S., and W. Hazeleger, 2001: Eddy mixing of potential vorticity versus thickness in an isopycnic ocean model. *J. Phys. Oceanogr.,* **31,** 481–505.

Eden, C., 2007: Eddy length scales in the North Atlantic Ocean. *J. Geophys. Res.,* **112,** C06004, doi:10.1029/2006JC003901.

Ferrari, R., 2006: Climate process team on eddy mixed layer interactions: Eddy-mixed layer interactions in the ocean. U.S. CLIVAR Variations, Vol. 4, No. 1, 2–4. [Available online at http://www.atmos.washington.edu/~breth/CPT-public/CPT-Variations-Wi06.pdf.]

——, and D. L. Rudnick, 2000: Thermohaline structure of the upper ocean. *J. Geophys. Res.,* **105C,** 16 857–16 883.

——, and A. Plumb, 2003: Residual circulation in the ocean. *Near-Boundary Processes and Their Parameterization: Proc. 'Aha Huliko'a Hawaiian Winter Workshop,* Honolulu, HI, University of Hawaii at Manoa, 219–228.

Ferreira, D., J. Marshall, and P. Heimbach, 2005: Estimating eddy stresses by fitting dynamics to observations using a residual-mean ocean circulation model and its adjoint. *J. Phys. Oceanogr.,* **35,** 1891–1910.

Fox-Kemper, B., and R. Ferrari, 2008: Parameterization of mixed

layer eddies. Part II: Prognosis and impact. *J. Phys. Oceanogr.,* **38,** 1166–1179.
——, ——, and B. Hallberg, 2008: Parameterization of mixed layer eddies. Part I: Theory and diagnosis. *J. Phys. Oceanogr.,* **38,** 1145–1165.
Garrett, C., 2001: Stirring and mixing: What are the rate-controlling processes? *From Stirring to Mixing in a Stratified Ocean: Proc. 'Aha Huliko'a Winter Workshop,* Honolulu, HI, University of Hawaii at Manoa, 1–8.
Gent, P. R., and J. C. McWilliams, 1990: Isopycnal mixing in ocean circulation models. *J. Phys. Oceanogr.,* **20,** 150–155.
Gerdes, R., C. Köberle, and J. Willebrand, 1991: The influence of numerical advection schemes on the results of ocean general circulation models. *Climate Dyn.,* **5,** 211–226.
Gnanadesikan, A., S. M. Griffies, and B. L. Samuels, 2007: Effects in a climate model of slope tapering in neutral physics schemes. *Ocean Modell.,* **16,** 1–16.
Greatbatch, R. J., and K. G. Lamb, 1990: On parameterizing vertical mixing of momentum in non-eddy-resolving ocean models. *J. Phys. Oceanogr.,* **20,** 1634–1637.
——, and G. Li, 2000: Alongslope mean flow and an associated upslope bolus flux of tracer in a parameterization of mesoscale turbulence. *Deep-Sea Res. I,* **47,** 709–735.
Gregg, M. C., T. B. Sanford, and D. P. Winkel, 2003: Reduced mixing from the breaking of internal waves in equatorial waters. *Nature,* **422,** 513–515.
Griffies, S., 2004: *Fundamentals of Ocean Climate Models*. Princeton University Press, 518 pp.
——, and Coauthors, 2005: Formulation of an ocean model for global climate simulations. *Ocean Sci.,* **1,** 45–79.
Haine, T. W. N., and J. Marshall, 1998: Gravitational, symmetric and baroclinic instability of the ocean mixed layer. *J. Phys. Oceanogr.,* **28,** 634–658.
Hallberg, R., and A. Gnanadesikan, 2006: The role of eddies in determining the structure and response of the wind-driven Southern Hemisphere overturning: Results from the Modeling Eddies in the Southern Ocean (MESO) project. *J. Phys. Oceanogr.,* **36,** 2232–2252.
Held, I. M., and T. Schneider, 1999: The surface branch of the zonally averaged mass transport circulation in the troposphere. *J. Atmos. Sci.,* **56,** 1688–1697.
Joyce, T. M., 1977: A note on the lateral mixing of water masses. *J. Phys. Oceanogr.,* **7,** 626–629.
Killworth, P. D., 1997: On the parameterization of eddy transfer. Part I: Theory. *J. Mar. Res.,* **55,** 1171–1197.
——, 2001: Boundary conditions on quasi-Stokes velocities in parameterizations. *J. Phys. Oceanogr.,* **31,** 1132–1155.
Kraus, E. B., and J. S. Turner, 1967: A one-dimensional model of the seasonal thermocline. II. The general theory and its consequences. *Tellus,* **19,** 98–105.
Kuo, A., R. A. Plumb, and J. Marshall, 2005: Transformed Eulerian-mean theory. Part II: Potential vorticity homogenization and the equilibrium of a wind- and buoyancy-driven zonal flow. *J. Phys. Oceanogr.,* **35,** 175–187.
Large, W. G., J. C. McWilliams, and S. C. Doney, 1994: Oceanic vertical mixing: A review and a model with a nonlocal boundary layer parameterization. *Rev. Geophys.,* **32,** 363–403.
——, G. Danabasoglu, S. C. Doney, and J. C. McWilliams, 1997: Sensitivity to surface forcing and boundary layer mixing in a global ocean model: Annual-mean climatology. *J. Phys. Oceanogr.,* **27,** 2418–2447.
——, ——, J. C. McWilliams, P. R. Gent, and F. O. Bryan, 2001: Equatorial circulation of a global ocean climate model with anisotropic horizontal viscosity. *J. Phys. Oceanogr.,* **31,** 518–536.
Larichev, V. D., and I. M. Held, 1995: Eddy amplitudes and fluxes in a homogeneous model of fully developed baroclinic instability. *J. Phys. Oceanogr.,* **25,** 2285–2297.
Ledwell, J. R., A. J. Watson, and C. S. Law, 1993: Evidence for slow mixing across the pycnocline from an open-ocean tracer-release experiment. *Nature,* **364,** 701–703.
Legg, S., J. C. McWilliams, and J. Gao, 1998: Localization of deep ocean convection by a mesoscale eddy. *J. Phys. Oceanogr.,* **28,** 944–970.
Marshall, D., 1997: Subduction of water masses in an eddying ocean. *J. Mar. Res.,* **55,** 201–222.
Marshall, J., and T. Radko, 2003: Residual-mean solutions for the Antarctic Circumpolar Current and its associated overturning circulation. *J. Phys. Oceanogr.,* **33,** 2341–2354.
——, A. Adcroft, C. Hill, L. Perelman, and C. Heisey, 1997: A finite-volume, incompressible Navier Stokes model for studies of the ocean on parallel computers. *J. Geophys. Res.,* **102,** 5753–5766.
McDougall, T. J., and P. C. McIntosh, 2001: The temporal-residual-mean velocity. Part II: Isopycnal interpretation and the tracer and momentum equations. *J. Phys. Oceanogr.,* **31,** 1222–1246.
McWilliams, J. C., 2003: Diagnostic force balance and its limits. *Nonlinear Processes in Geophysical Fluid Dynamics,* O. U. Velasco Fuentes, J. Sheinbaum, and J. Ochoa, Eds., Kluwer, 287–304.
Mellor, G. L., and T. Yamada, 1974: A hierarchy of turbulence closure models for planetary boundary layers. *J. Atmos. Sci.,* **31,** 1791–1806.
Oschlies, A., 2002: Improved representation of upper-ocean dynamics and mixed layer depths in a model of the North Atlantic on switching from eddy-permitting to eddy-resolving grid resolution. *J. Phys. Oceanogr.,* **32,** 2277–2298.
Paiva, A. M., J. T. Hargrove, E. P. Chassignet, and R. Bleck, 1999: Turbulent behavior of a fine mesh (1/12°) numerical simulation of the North Atlantic. *J. Mar. Syst.,* **21,** 307–320.
Plumb, R. A., and R. Ferrari, 2005: Transformed Eulerian-mean theory. Part I: Nonquasigeostrophic theory for eddies on a zonal-mean flow. *J. Phys. Oceanogr.,* **35,** 165–174.
Pollard, R. T., M. J. Griffiths, S. A. Cunningham, J. F. Read, F. F. Pérez, and A. F. Ríos, 1996: Vivaldi 1991—A study of the formation, circulation, and ventilation of eastern North Atlantic central water. *Prog. Oceanogr.,* **37,** 167–192.
Price, J. F., 2001: Subduction. *Ocean Circulation and Climate: Observing and Modelling the Global Ocean,* G. Siedler, J. Church, and J. Gould, Eds., Academic Press, 357–371.
——, R. A. Weller, and R. Pinkel, 1986: Diurnal cycling: Observations and models of the upper ocean response to diurnal heating, cooling, and wind mixing. *J. Geophys. Res.,* **91,** 8411–8427.
Redi, M. H., 1982: Oceanic isopycnal mixing by coordinate rotation. *J. Phys. Oceanogr.,* **12,** 1154–1158.
Robbins, P. E., J. F. Price, W. B. Owens, and W. J. Jenkins, 2000: The importance of lateral diffusion for the ventilation of the lower thermocline in the subtropical North Atlantic. *J. Phys. Oceanogr.,* **30,** 67–89.
Roberts, M., and D. Marshall, 1998: Do we require adiabatic dissipation schemes in eddy-resolving ocean models? *J. Phys. Oceanogr.,* **28,** 2050–2063.
Scott, R. B., and F. Wang, 2005: Direct evidence of an oceanic

inverse kinetic energy cascade from satellite altimetry. *J. Phys. Oceanogr.,* **35,** 1650–1666.

Smagorinsky, J., 1963: General circulation experiments with the primitive equations: I. The basic experiment. *Mon. Wea. Rev.,* **91,** 99–164.

Smith, R. D., and J. C. McWilliams, 2003: Anisotropic horizontal viscosity for ocean models. *Ocean Modell.,* **5,** 129–156.

——, and P. R. Gent, 2004: Anisotropic Gent–McWilliams parameterization for ocean models. *J. Phys. Oceanogr.,* **34,** 2541–2564.

——, M. E. Maltrud, F. O. Bryan, and M. W. Hecht, 2000: Numerical simulation of the North Atlantic Ocean at 1/10°. *J. Phys. Oceanogr.,* **30,** 1532–1561.

Sneddon, I. N., 1957: *Elements of Partial Differential Equations*. McGraw-Hill, 327 pp.

Solomon, H., 1971: On the representation of isentropic mixing in ocean circulation models. *J. Phys. Oceanogr.,* **1,** 233–234.

Stammer, D., 1997: Global characteristics of ocean variability from regional TOPEX/POSEIDON altimeter measurements. *J. Phys. Oceanogr.,* **27,** 1743–1769.

Toole, J. M., R. W. Schmitt, and K. L. Polzin, 1994: Estimates of diapycnal mixing in the abyssal ocean. *Science,* **264,** 1120–1123.

Treguier, A. M., I. M. Held, and V. D. Larichev, 1997: Parameterization of quasi-geostrophic eddies in primitive equation ocean models. *J. Phys. Oceanogr.,* **27,** 567–580.

Visbeck, M., J. Marshall, T. Haine, and M. Spall, 1997: On the specification of eddy transfer coefficients in coarse-resolution ocean circulation models. *J. Phys. Oceanogr.,* **27,** 381–402.

Wardle, R., and J. Marshall, 2000: Representation of eddies in primitive equation models by a PV flux. *J. Phys. Oceanogr.,* **30,** 2481–2503.

Weller, R. A., 2003: Subduction. *Near-Boundary Processes and Their Parameterization: Proc. 'Aha Huliko'a Hawaiian Winter Workshop,* Honolulu, HI, University of Hawaii at Manoa, 171–176.

Wunsch, C., 1997: The vertical partition of oceanic horizontal kinetic energy. *J. Phys. Oceanogr.,* **27,** 1770–1794.

Young, W. R., 1994: The subinertial mixed layer approximation. *J. Phys. Oceanogr.,* **24,** 1812–1826.